Functionalized Nanotubes

DOI: 10.1002/anie.200901658

Defect-Mediated Functionalization of Carbon Nanotubes as a Route to Design Single-Site Basic Heterogeneous Catalysts for Biomass Conversion**

Jean-Philippe Tessonnier, Alberto Villa, Olivier Majoulet, Dang Sheng Su, and Robert Schlögl*

The use of biomass will play a key role in the production of chemicals over the next few decades.[1–3] It is estimated that 25% of the chemicals in the US will be produced from biomass by 2030,[2] and it is therefore clear that billions of tons of biomass-based chemicals will have to be synthesized. This goal constitutes a real challenge for heterogeneous catalysis as its focus will have to move from the well-known C–C bond chemistry (cracking, isomerization, and alkylation) to C–O bond chemistry (e.g., dehydration and deoxygenation). Therefore, the chemistry of carbohydrates needs to be explored and developed.[4] In this context, basic heterogeneous catalysts will play a major role in, for example, dehydration, hydrolysis, (trans)esterification, aldol condensation, alkylation, or isomerization reactions.[1,3] At present, basic heterogeneous catalysts usually consist of alkaline oxides, alkaline-earth oxides, clays, and modified zeolites.[1,5] However, they present different drawbacks such as the low number of accessible active sites, important diffusion and mass transfer problems, or partial dissolution in the reaction medium for applications in liquid-phase biomass conversion.[6] It is therefore necessary to develop new basic heterogeneous catalysts that are highly selective, stable, and easy to tailor on a nano and macro level. Multiwall carbon nanotube (MWCNT) based catalysts fit each of these criteria. They are chemically stable in most media, present a high surface area, and can be directly grown in self-standing blocks by controlling the entanglement of the nanotubes.[7] In addition, many of the reactions known in organic chemistry can be employed to chemically modify MWCNTs, for example, by grafting specific functional groups onto their surface.[8–11] In this way, we believed it should be possible to tailor single-site MWCNT-based catalysts that are highly selective. Herein, we report a novel approach to the synthesis of MWCNT-grafted amino groups by modifying existing structural defects of the MWCNTs. The catalysts were tested in the synthesis of biodiesel as a model reaction for applications in C–O chemistry, that is, biomass conversion reactions. The stability of the basic functional groups during the catalytic reaction as a function of the synthetic route employed for their grafting is discussed.

The most common synthetic route to functionalized MWCNTs is based on the reactivity of surface carboxyl groups. Single-wall or multiwall carbon nanotubes are first oxidized with nitric acid to create carboxylic acid moieties on their surfaces. Coupling and anchoring of the desired molecule is then performed by, for example, amidation (Scheme 1), esterification, or Friedel–Crafts reactions.[8]

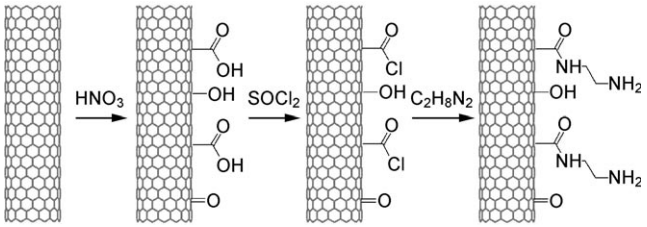

Scheme 1. Functionalization of MWCNTs by oxidation–amidation.

Although this oxidation–coupling technique is very popular, it suffers from several drawbacks. It was shown that MWCNTs are shortened during the oxidation step, which could make recovery of the catalyst after reaction more difficult. In addition, the oxidation step also creates a variety of other acidic oxygen-containing groups (see the Supporting Information),[12] which remain in the final sample and are prone to adsorb and react with biomass constituents during the catalytic reaction. These side-reactions lower the selectivity for the desired products and can even irreversibly poison the catalyst. In order to circumvent these problems, we developed a more elegant and more efficient synthetic route based on the direct covalent grafting of the desired basic functional groups onto existing structural defects of the MWCNTs. Contrary to the case of graphite, structural defects are common for nanotubes, especially for MWCNTs grown by catalytic chemical vapor deposition (CCVD). Ideal carbon nanotubes are straight along their main axis.[13] However, scanning electron microscopy (SEM; see the Supporting Information) and transmission electron microscopy (TEM) images clearly show that MWCNTs are curved, which implies that they contain many topological defects where one or several hexagons have been replaced by pentagons and heptagons.[13] The intensity of the D band and the D/G ratio in the Raman spectra of the MWCNTs (where D and G are the

[*] Dr. J.-P. Tessonnier, Dr. A. Villa, O. Majoulet, Dr. D. S. Su, Prof. R. Schlögl
Department of Inorganic Chemistry
Fritz Haber Institute of the Max Planck Society
Faradayweg 4–6, Berlin (Germany)
Fax: (+49) 30-8413-4401
http://www.fhi-berlin.mpg.de
E-mail: tesso@fhi-berlin.mpg.de

[**] We acknowledge Süd Chemie as well as the Federal Ministry of Education and Research (Carboscale) for their support.

Supporting information for this article is available on the WWW under http://dx.doi.org/10.1002/anie.200901658.

disorder-induced and graphite bands, respectively) can indicate the existence of structural defects, such as point defects, dislocations, and especially vacancies. SWCNTs synthesized by arc discharge have very few defects and therefore exhibit a D/G ratio below 1. In comparison, the commercially available MWCNTs used here are significantly more defective (see the Supporting Information). The large number of chemically reactive vacancies and sp^3 carbon atoms can therefore be used for the covalent attachment of desired molecules onto the sidewalls by C–C coupling reactions.

In our synthetic route (Scheme 2), MWCNTs are first reacted with an excess of *n*BuLi, which is a strong base as well as a good nucleophile. C–H bonds located near defects can be deprotonated and replaced by C–Li bonds. In parallel, *n*BuLi

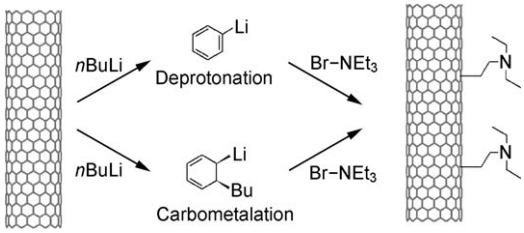

Scheme 2. Functionalization of MWCNTs by deprotonation–carbometalation and subsequent electrophilic attack of the bromotriethylamine.

can also react with the MWCNTs through the carbometalation reaction, which is a common reaction known to proceed through a local break in the aromatic system. This reaction is difficult, but occurs for polyaromatic species because of their ability to delocalize and thus stabilize the negative charge that is created. Carbometalation reactions were also successfully performed on fullerenes and SWCNTs. A significant increase in the D band of SWCNTs showed that the functionalization took place on the sidewall, thus creating a new defect with a sp^3 carbon atom.[14] SWCNTs typically have a small diameter that induces strain and therefore pyramidalization of the carbon atoms and misalignment of the π orbitals.[10] For both C_{60} and SWCNTs, the covalent attachment of addends is favored by the rehybridization of a network carbon atom to sp^3 and the consequent reduction of the strain energy. Pyramidalization is much lower for SWCNTs than for C_{60}, which explains the lower reactivity of SWCNTs (see the Supporting Information).[10,15–17] The diameter and therefore the curvature of MWCNTs is far larger than for SWCNTs. For example, the Nanocyl MWCNTs used in this work have an external diameter of approximately 10 nm. The reactivity of the sidewalls is far lower than that of SWCNTs, therefore, it is very likely that the carbometalation reaction only occurs on defects, for example, localized C=C bonds and Stone–Wales defects. In the second step of our synthetic route, 2-diethylaminoethylbromide was added to the activated MWCNTs in order to perform an electrophilic attack on the C–Li bond (Scheme 2). A new C–C bond is formed between the ethyl group of the amine and the MWCNT, thus leading to a covalent functionalization of the nanotube with triethylamine and formation of LiBr as a by-product.

Characterization of functionalized carbon nanotubes with the traditional tools employed in organic chemistry such as NMR, IR, or UV/Vis spectroscopy is extremely difficult, as already reported by Graupner et al.[14] XPS cannot be applied because of the possible photolysis of the amino groups under X-ray exposure.[18] Instead, we used a set of different techniques such as electron microscopy, porosimetry, Raman spectroscopy, thermogravimetry (TG), and acid–base titrations in order to investigate possible changes in the structure of the MWCNTs and to quantify the anchored groups. Another sample, which was prepared by the common oxidation–amidation route[19] (Scheme 1), was used for comparison. SEM images of both samples (see the Supporting Information) do not show any amorphous carbon, carbon particles, or other carbon impurities. Both samples are homogeneous, which simplifies the interpretation of the results obtained from other characterization techniques and make them more reliable. The presence of nitrogen in both samples was confirmed by energy-dispersive X-ray spectroscopy (EDX). The nitrogen peak for the sample prepared by oxidation–amidation is higher than that of the sample prepared by using our electrophilic attack method (see the Supporting Information). This result is consistent with previous reports on the efficiency of this grafting technique. A sharp oxygen peak was also observed for the sample obtained by oxidation–amidation; this result is consistent with the first step of oxidation with nitric acid and the anchoring of the diamine by amidation. Surprisingly, sulfur was also found to be present in this sample. It appears that additional reactions take place during the acylation step with $SOCl_2$ and that sulfur-containing groups are either adsorbed or anchored on the surface of the MWCNTs. The sample prepared by using our method only shows traces of oxygen and bromine.

HRTEM images (Figure 1) and Raman spectra (see the Supporting Information) further confirm that the structure of

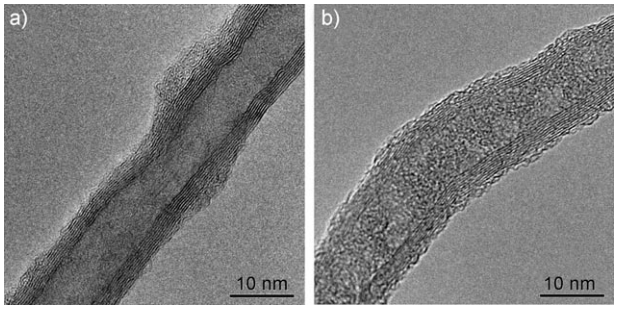

Figure 1. HRTEM images of the samples prepared by a) electrophilic attack and b) the common oxidation–amidation route.

the MWCNTs has not been altered for both samples. The Raman spectrum of the sample prepared by oxidation–amidation shows slightly broader peaks and a slightly higher D/G ratio than the sample prepared by electrophilic attack, as additional defects were created, probably during the oxidation step with nitric acid. HRTEM images of the sample prepared by our procedure are similar to those of the pristine MWCNTs; small amorphous deposits were found on some of

the nanotubes (Figure 1a). However, in general, functional groups could not be observed, which was expected as the individual groups are too small to be imaged and as there is no crystallographic ordering of the surface groups. Reciprocally, Figure 1a indirectly confirms that the amino groups are well dispersed on the surface. High dispersion and accessibility of the active sites are two important parameters that must be fulfilled to reach a high activity in catalysis. In contrast, for the sample prepared by oxidation–amidation (Figure 1b), an amorphous or highly disordered coating is observed around the MWCNTs and inside their channels. The pore-size distribution obtained from porosimetry measurements (see the Supporting Information) indicates that the contribution from pores smaller than 5 nm, that is, the inner diameter of the nanotubes, disappeared for the oxidation–amidation sample. Clearly, the inner channels of the MWCNTs were filled and blocked by the deposits, thus leading to a loss of 50% of the surface area of the nanotubes. The functionalization by electrophilic attack seems more efficient. The pore-size distribution of MWCNTs prepared by using this method shows almost no difference when compared to the pristine MWCNTs; this result indicates that the functional groups homogeneously coat the inner and outer walls of the nanotubes. The contribution from larger mesopores, which originate from the entanglement of the nanotubes,[20] decreased for both samples. Other research groups have already shown that SWCNTs can be debundled when functionalizing their surfaces.[21] In a similar way, the functionalization partially disentangles the MWCNTs, thus leading to fewer pores with diameters between 10 and 100 nm.

The efficiency of both procedures to graft desired functional groups on the nanotube surface was evaluated by thermogravimetry/mass spectrometry (TG-MS) as well as by acid–base titrations. The TG-MS curves (Figure 2) do not show any weight loss below 130 °C, that is, at the boiling points of triethylamine and ethylenediamine, thus proving that the amines were successfully anchored on the MWCNTs. The weight loss proceeded in two steps for the NEt_3–MWCNT sample prepared by electrophilic attack. For each step, only fragments characteristic of the amines were detected by mass spectrometry (see the Supporting Information). It appears that amino groups anchored on different defects exhibit a different thermal stability. While 39% of the functional groups were lost between 130 °C and 570 °C, a full 61% are stable up to 570 °C. The total weight loss at 900 °C was 10%, which represents 1.10^{-3} mol of anchored triethylamine groups per gram of MWCNTs and therefore approximately two amino groups per nm^2. The NH_2–MWCNT sample prepared by oxidation–amidation exhibits a significantly higher weight loss of about 42% at 900 °C. A significant amount of water was lost between room temperature and 400 °C (see the Supporting Information). This relatively high temperature indicates that the water was certainly trapped by the amorphous deposits inside the MWCNTs (Figure 1b). The evolution of the signal at m/z 30, which is characteristic of ethylenediamine, indicates that the decomposition of the grafted groups starts at 200 °C and becomes significant at 550 °C. The amount and the basicity of the anchored groups were further characterized by acid–base titrations (Figure 3). The initial pH of the NEt_3–MWCNTs suspended in water was

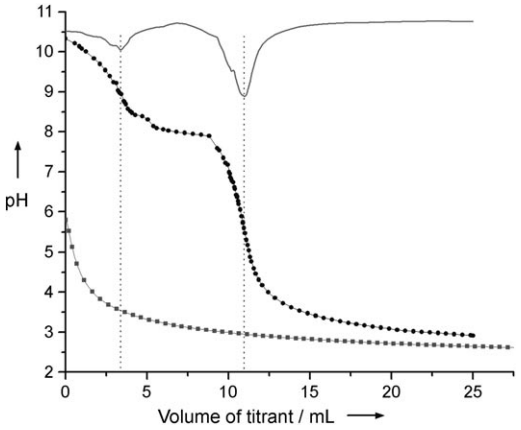

Figure 3. Titration curves of the basic groups anchored on the samples synthesized by electrophilic attack (● NEt_3–MWCNT) and by the common oxidation–amidation route (■ NH_2–MWCNT) The first-derivative curve (——) indicates the position of the two equivalence points for the NEt_3–MWCNT sample.

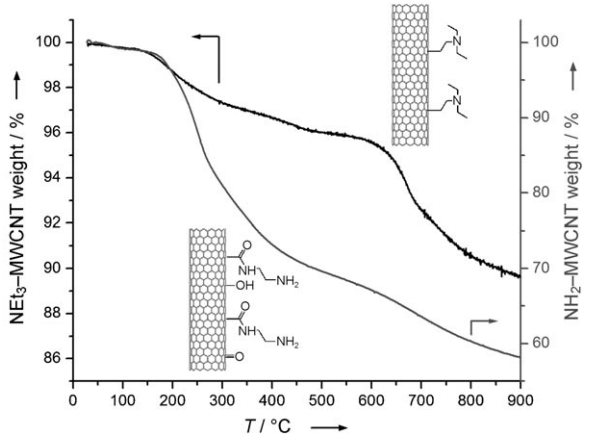

Figure 2. TG curves of the samples prepared by electrophilic attack (NEt_3–MWCNT) and by oxidation–amidation (NH_2–MWCNT).

10.3. Two equivalence points were observed, and pK_{a_1} and pK_{a_2} were found to be 9.9 and 8.1, respectively. The total number of basic groups was found to be 1.10^{-3} mol g^{-1}, which is in good agreement with the TG-MS data. From the equivalence points, we calculated that the groups with pK_{a_1} and pK_{a_2} represent 31% and 69% of the basic groups, respectively. The ratio of these values is consistent with the two main weight losses measured by TG-MS. The origins of these differences in basicity and thermal stability are not yet clear, although steric hindrance of neighboring groups or influence from the nanotube surface may be possible reasons. The correlation of TG-MS and titration results confirms that our procedure leads to a selective grafting of triethylamine groups onto the surface of the MWCNTs. For comparison, the sample synthesized by oxidation–amidation had a starting pH of 5.8, which confirmed the coexistence of basic amino groups with a large number of acidic sulfur- and oxygen-containing

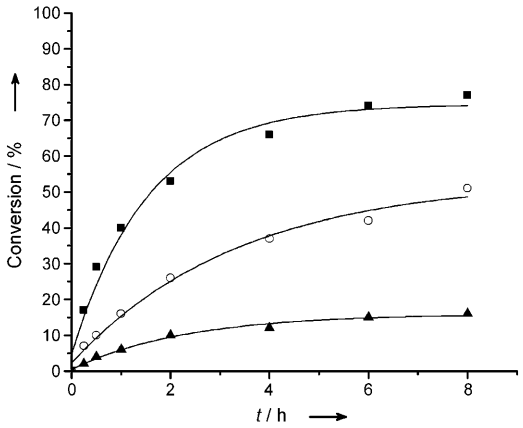

Figure 4. Triglyceride conversion as a function of time obtained for the samples prepared by electrophilic attack (■ NEt_3–MWCNT) and by the common oxidation–amidation route (▲ NH_2–MWCNT), as well as for a commercial hydrotalcite (○).

groups. XPS analysis revealed that the concentration of oxygen-containing groups was as high as 9 atomic percent.

Both samples were tested as potential basic heterogeneous catalysts for biomass conversion reactions. Their catalytic activity was evaluated for the transesterification of glyceryl tributyrate with methanol, which is considered as a test reaction for the production of biodiesel.[22] We compared our results with a commercial hydrotalcite, which is a standard catalyst for this reaction (Figure 4).[22] The target ester methyl butanoate was always found to be the main product, and the diglyceride and monoglyceride, which are the reaction intermediates, were less than a few percent of the products. The catalyst prepared by using our procedure gave a conversion of 77% after 8 hours. For comparison, the hydrotalcite tested under the same conditions gave only 51% conversion. Importantly, Li was not detected by inductively coupled plasma atomic emission spectroscopy (ICP-AES), and therefore the high activity of the NEt_3–MWCNT catalyst cannot be attributed to Li impurities that originate from the BuLi employed in the synthesis.

The lowest conversion was obtained with the sample prepared by oxidation–amidation. Although the grafted amino groups are basic enough to catalyze the transesterification reaction, this catalyst showed a poor activity and a high deactivation. Transesterification reactions are catalyzed both by acids and bases. However, the proximity of both remaining acidic oxygen-containing groups and basic amino groups in this sample allow them to neutralize each other, as observed by acid–base titration. Therefore, there are fewer active sites available to catalyze the transesterification reaction, which explains the low triglyceride conversion observed. In addition, deactivation by poisoning as well as leaching of the surface amino groups cannot be excluded. This test demonstrates that the synthetic route used for the covalent grafting of amino groups plays a key role in the catalytic activity of the synthesized material.

In summary, we have demonstrated that amino groups can be grafted on MWCNTs by a simple, one-pot, deprotonation–carbometalation reaction followed by an electrophilic substitution. This procedure is faster and more elegant that the classical oxidation–amination route, which involves several steps and requires harsh reagents. Our synthetic route leads to very homogeneous samples with a high number of easily accessible basic groups. The concentration of the functional groups, without any optimization of the grafting procedure, was found to be 1 $mmol\,g^{-1}$, which is close to the concentration of Brønsted acid sites in zeolites. A high catalytic activity was measured for a model biomass conversion reaction. The catalytic activity and the stability under reaction conditions of these samples will be reported in detail elsewhere.

Received: March 26, 2009
Revised: June 30, 2009
Published online: July 23, 2009

Keywords: biomass · electrophilic substitution · heterogeneous catalysis · nanotubes · sustainable chemistry

[1] A. Corma, S. Iborra, A. Velty, *Chem. Rev.* **2007**, *107*, 2411 – 2502.
[2] G. W. Huber, S. Iborra, A. Corma, *Chem. Rev.* **2006**, *106*, 4044 – 4098.
[3] P. Mäki-Arvela, B. Holmbom, T. Salmi, D. Y. Murzin, *Catal. Rev. Sci. Eng.* **2007**, *49*, 197 – 340.
[4] Juben N. Chheda, George W. Huber, James A. Dumesic, *Angew. Chem.* **2007**, *119*, 7298 – 7318; *Angew. Chem. Int. Ed.* **2007**, *46*, 7164 – 7183.
[5] A. M. Ruppert, Johannes D. Meeldijk, B. W. M. Kuipers, Ben H. Erné, Bert M. Weckhuysen, *Chem. Eur. J.* **2008**, *14*, 2016 – 2024.
[6] Y. Liu, E. Lotero, J. J. G. Goodwin, C. Lu, *J. Catal.* **2007**, *246*, 428 – 433.
[7] J. Amadou, D. Begin, P. Nguyen, J. P. Tessonnier, T. Dintzer, E. Vanhaecke, M. J. Ledoux, C. Pham-Huu, *Carbon* **2006**, *44*, 2587 – 2589.
[8] D. Tasis, N. Tagmatarchis, A. Bianco, M. Prato, *Chem. Rev.* **2006**, *106*, 1105 – 1136.
[9] Y. P. Sun, K. Fu, Y. Lin, W. Huang, *Acc. Chem. Res.* **2002**, *35*, 1096 – 1104.
[10] S. Niyogi, M. A. Hamon, H. Hu, B. Zhao, P. Bhowmik, R. Sen, M. E. Itkis, R. C. Haddon, *Acc. Chem. Res.* **2002**, *35*, 1105 – 1113.
[11] A. Hirsch, O. Vostrowsky in *Functional Organic Materials*, *Vol. 1* (Eds.: T. J. J. Müller, U. H. F. Bunz), Wiley-VCH, Weinheim, **2007**.
[12] H. P. Boehm, E. Diehl, W. Heck, R. Sappok, *Angew. Chem.* **1964**, *76*, 742 – 751; *Angew. Chem. Int. Ed. Engl.* **1964**, *3*, 669 – 677.
[13] J. C. Charlier, *Acc. Chem. Res.* **2002**, *35*, 1063 – 1069.
[14] R. Graupner, J. Abraham, D. Wunderlich, A. Vencelova, P. Lauffer, J. Rohrl, M. Hundhausen, L. Ley, A. Hirsch, *J. Am. Chem. Soc.* **2006**, *128*, 6683 – 6689.
[15] Z. Chen, W. Thiel, A. Hirsch, *ChemPhysChem* **2003**, *4*, 93 – 97.
[16] D. Wunderlich, F. Hauke, A. Hirsch, *J. Mater. Chem.* **2008**, *18*, 1493 – 1497.
[17] D. Wunderlich, F. Hauke, A. Hirsch, *Chem. Eur. J.* **2008**, *14*, 1607 – 1614.
[18] P. J. Kozak, H. Gesser, *J. Chem. Soc.* **1960**, 448 – 452.
[19] B. Pan, D. Cui, F. Gao, R. He, *Nanotechnology* **2006**, *17*, 2483 – 2489.
[20] A. Peigney, C. Laurent, E. Flahaut, R. R. Bacsa, A. Rousset, *Carbon* **2001**, *39*, 507 – 514.
[21] J. Chen, M. A. Hamon, H. Hu, Y. Chen, A. M. Rao, P. C. Eklund, R. C. Haddon, *Science* **1998**, *282*, 95 – 98.
[22] D. G. Cantrell, L. J. Gillie, A. F. Lee, K. Wilson, *Appl. Catal. A* **2005**, *287*, 183 – 190.

